Palladium Decorated SWCNTs Sensor for Detecting Methane at Room Temperature Based on UWB-RFID

Jian Liu and Ping B. Li

School of Communication and Information Engineering
Xi'an University of Science and Technology, Xi'an, 710054, China
liujian2@xust.edu.cn, lbp90128@xust.edu.cn

Abstract ─ A chipless sensor in the protocol of ultra wideband radio frequency identification (UWB-RFID) is proposed in the paper. This sensor, used to detect methane at room temperature, is configured by a planar patch antenna plus a U slot on which interdigitated fingers electrodes (IDE) with load of palladium decorated single walled carbon nanotubes (Pd-SWCNTs) are embedded. The sensor can cover the entire UWB spectrum except for the band that produce band-gap. The amplitudes and frequencies of the band-gap are designated as the signatures modulated and reflecting the status quo of methane retrieved by Pd-SWCNTs. The sensor is validated by an approximate combination of the analytical and numerical method. Results show that if the concentration of methane is increased from 0 ppm to 100 ppm at room temperature, the *identifiable sensitivity* can be achieved by -9.32 dB in terms of the scheme of the amplitude modulation of band-gap frequency; or, the *identifiable sensitivity* can be achieved by -11.30 dB in terms of the scheme of the frequency modulation of band-gap frequency.

Index Terms ─ Chipless tag, methane sensor, nano-technology, room temperature, ultra-wideband radio frequency identification (UWB-RFID).

I. INTRODUCTION

The exploration of safe and accurate method to detect methane at room temperature is a critical issue due to the fact that methane, once concentrated in air by 4%, can cause combustion, or even explosion. Some traditional methods like the catalytic beads, the metal oxides and the infrared flame ionizations are readily used to detect the concentration of methane, but they needs to consume a large amount of energy, and the required environmental temperature is usually high up to 500°C [1]. This situation is changed since the single walled carbon nanotubes (SWCNTs) was invented in 1990s. It is these sensors that are decorated by the single walled carbon nanotubes can really make detecting methane at room temperature possible [2].

Additionally, the detection of methane in the consideration of safety issue is firmly relevant to the way of contactless intrusion to the methane's molecule, the protocol of wireless communication is therefore a pivotal in this regards. Commonly, the wireless sensor networks (WSN) is an amazing choice for its longer lifetime and lower complexity, and it is more specific if the sensor node is the sort of chipless type (tag) that is nothing but to be interrogated by reader passively or semi-actively [3].

On this account, the radio frequency identification (RFID) is a more appropriate protocol for the WSN in specific for the case that all the sensors are the type of chipless tags. A few of such applications have been implemented and released in recent literatures [4-7]. However, we find that all the RFID mentioned here are the narrow band circumstances borne with narrow band characteristics, for example, the interrogation signals are the sort of standardized continuous waves. As a result, these systems are common in weakness in canceling the multipath effects; and the sensor tags are more vulnerable in fighting against narrowband and multiuser interference with lower security. So, the narrow band RFID is not regarded as a promising wireless framework for the future identification where higher level reliability for real-time identification and intensive accuracy for positioning in sub-meters level are awfully required [8].

However, this narrow band RFID could be replaced by broader band counterpart if combing RFID with the technology of ultra-wide band, known as UWB-RFID. In a UWB-RFID system, a very short pulse will take over the standard continuous wave to conduct tag interrogation. This way could make transceiver in UWB-RFID to consume less power on one hand; the other hand, it could make tags serve to positioning in accuracy of sub-meter level. Furthermore, tags in UWB-RFID perform more robustness in fighting against multipath interference and have large coverage area, low detection probability and solid security. In the meanwhile, they can be more effective in improving the accessibility of multiple channels and making interference be mitigated a great deal [9].

In theory, when a UWB-RFID uses a very short

Submitted On: September 22, 2015
Accepted On: May 3, 2016

pulse as the signal of interrogation, it will leave two types of pulses existed in the backscattering waves with one called the structural mode; and another the antenna mode. Referring to the investigations unveiled in recent literatures [10-12], we can find that almost all the tags concerned are governed solely by the antenna mode or by the spectrum of backscattering signals, few of them are purely on the structural mode even if the structural mode has been verified to be possess of less pulse deformation against the waveform of interrogation pulse, and the amplitude of structural mode is accordingly larger than that of the antenna mode [13].

So, in this paper, we propose a design of UWB-RFID chipless tag in specific for detecting methane at room temperature. The mechanism of the detection is based on the signature intended in the structural mode only. The configuration of tag is a combination of a metallic portrayed electromagnetic interface with a sensor head made from interdigitated fingers electrodes (IDE) loaded by palladium decorated single walled carbon nanotubes (Pd-SWCNTs). The performance of the tag is described by the parameter of *identifiable sensitivity* that will be defined and derived in the paper.

II. UWB-RFID SENSOR SYSTEM

A typical UWB-RFID sensor system consists of a reader and a sensor node, as shown in Fig. 1. The sensor node is the chipless type that is interrogated by reader passively or semi-actively. If the frequency is *f*, the modulus of $S_{11}(f)$ will represent the reflection coefficient of the reader antenna, $D_t(\theta_t, \emptyset_t)$ will represent the directivity of the reader antenna where θ_t and $\emptyset_t$ are the elevation and azimuth angle along which the interrogation signal is transmitted. Also shown in Fig. 1, the chipless tag consists of a sensor head and an antenna, the modulus of $S_{22}(f)$ represents the reflection coefficient of the tag antenna, $D_r(\theta_r, \emptyset_r)$ represents the directivity of the tag antenna where θ_r and $\emptyset_r$ are the elevation and azimuth angle along which the backscattering signal is received [14].

In Fig. 1, T_{rs} represents the structural mode, T_{rt} represents the antenna mode. In principle, the amplitude, frequency and time on both structural mode and antenna mode can be the candidate signatures used to convey the sensed information.

For achieving structural mode only, the load of the tag should be impedance match to the feed line. If P_t represents the power emitted by reader, P_r represents the power received by reader [15], we have:

$$\frac{P_r}{P_t} = e_t\left(1-\left|S_{11}(f)\right|^2\right)\frac{D_t(\theta_t,\phi_t)}{4\pi R_1^2} \times \sigma\frac{\lambda^2}{4\pi}\frac{D_r(\theta_r,\phi_r)}{4\pi R_2^2}e_r\left(1-\left|S_{22}(f)\right|^2\right), \tag{1}$$

where e_t and e_r are the loss coefficients that are associated with the performance of insertion loss and antenna efficiency. R_1 is the distance from reader to tag, R_2 is the reverse distance from tag and reader, λ is the wavelength, σ is the radar cross section (RCS).

For simplicity, the antenna in reader is same for transmission and reception, and it is also polarization matching to the tag antenna. R_1 is equal to R_2 denoted by R, $D_t(\theta_t, \emptyset_t)$ is equal to $D_r(\theta_r, \emptyset_r)$, then the structural mode $Y_s(f)$ is approximated to:

$$\begin{aligned} Y_S(f) \approx{}& X(f)\sqrt{\left(1-\left|S_{11}(f)\right|^2\right)} \\ &\times\sqrt{e_tD_t(\theta_t,\phi_t)}\frac{1}{\sqrt{4\pi}R}e^{-2j\pi f\frac{Rt}{c}} \\ &\times\sqrt{\sigma}\frac{c}{\sqrt{4\pi}|f|}\sqrt{e_rD_r(\theta_r,\phi_r)}\frac{1}{\sqrt{4\pi}R}e^{-2j\pi f\frac{Rt}{c}} \\ &\times\sqrt{\left(1-\left|S_{22}(f)\right|^2\right)}, \end{aligned} \tag{2}$$

where $X(f)$ is the pulse transmitted by reader in the domain of frequency, *c* is the wave velocity in free space.

The above equation can be rewritten as:

$$\begin{aligned} Y_S(f) \approx{}& X(f)\eta_T\sqrt{\left(1-\left|S_{11}(f)\right|^2\right)}H_F(f) \\ &\times\eta_L H_R(f)A(f)\eta_R\sqrt{\left(1-\left|S_{22}(f)\right|^2\right)}, \end{aligned} \tag{3}$$

where $\eta_T = \sqrt{e_tD_t(\theta_t,\phi_t)}$, $\eta_R = \sqrt{e_rD_r(\theta_r,\phi_r)}$, $H_F(f) = H_R(f) = (1)/(\sqrt{4\pi}R)e^{-2j\pi f(R)/(c)t}$, and $\eta_L = \sqrt{\sigma}$. The effective aperture of the antenna is $A(f) = c/(\sqrt{4\pi}|f|)$.

In (3), η_L and $\sqrt{\left(1-\left|S_{22}(f)\right|^2\right)}$ are the terms associated with the characteristics of tag. All the variants there can be designated as the signatures used to convey the sensed information including the intended information of the tag: the status quo of concentration of methane.

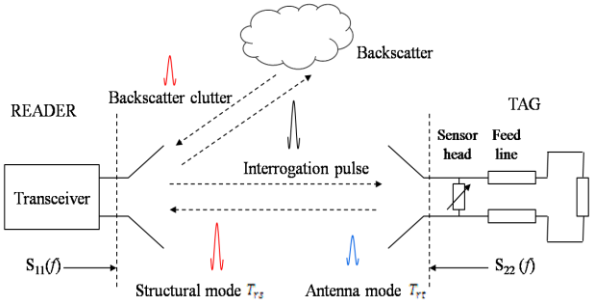

Fig. 1. The illustration of the mechanism of backscattering for the emitted pulse to interrogate chipless tag passively and semi-actively with presence of scatters.

III. UWB-RFID CHIPLESS TAG FOR DETECTING METHANE

It is evidence that the RCS σ and the reflection coefficient $|S_{22}(f)|$ are of importance to determine the

structure and the performance of the sensor tag. For chipless type, the sensor tag is usually composed of an electromagnetic interface and a sensor head. The electromagnetic interface is used to receive and backscatter the interrogation signal; however the sensor head is used to realize the specified sensing mechanism that will give the interrogation signal a kind of manipulation. So, the signatures dedicated by the electromagnetic interface should be capable of responding sensor head with a broad dynamic range so as to make tag be with of good sensitivity.

A. Electromagnetic interface

In the design, the electromagnetic interface is grown on a substrate that is a thinly filmed structure in order to facilitate geometry conformal to target object. The antenna of the electromagnetic interface is a planar patch with an arc typed edge, and the feed is micro-strip line connected by a load, as shown in Fig. 3 and Fig. 4 [16].

In the middle of the antenna plane, there is a U-slot etched to create a band-gap frequency in the backscattering spectrum [17]. The RCS $\sigma$and $|S_{22}(f)|$ are the function of the spectrum that are influenced by the depth (amplitude) and the location (frequency) of this band-gap frequency. If the signature is selected as the *amplitude* of the band-gap frequency, we define it the sensing scheme of the amplitude modulation of band-gap frequency; and if the signature is selected as the *frequency* of the band-gap frequency, we define it the sensing scheme of the frequency modulation of band-gap frequency.

Given $d(t)$ representing the function of the concentration of methane versus time, $Y_s(f)$ is the structural mode related both to the band-gap frequency *f* and $d(t)$ denoted by $Y_s[f, d(t)]$, the amplitude of band-gap frequency $Y_s[f, d(t)]$ can be expressed as:

$$Y_S[f, d(t)] \approx X(f)\eta_T\sqrt{(1-|S_{11}(f)|^2)}H_F(f) \times \eta_L[d(t)]H_R(f)A(f)\eta_R\sqrt{(1-|S_{22}[f, d(t)]|^2)}, \quad (4)$$

where $|S_{22}(f)|$ is replaced by $|S_{22}[f, d(t)]|$, indicating that the modulus of the reflection coefficient is dependent on the concentration of methane; $\eta_L = \sqrt{\sigma}$ is replaced by $\eta_L[d(t)] = \sqrt{\sigma[d(t)]}$, also indicating that the RCS is dependent on the concentration of methane.

The above equation can be rewritten as:

$$Y_S[f, d(t)] \approx X_f(f)Y_d[f, d(t)], \quad (5)$$

where $X_f(f) \approx X(f)\eta_T\sqrt{(1-|S_{11}(f)|^2)}H^2(f)A(f)\eta_R$ indicating the terms that are irrelevant to the concentration of methane. $Y_d[f, d(t)] = \eta_L[d(t)]\sqrt{(1-|S_{22}[f, d(t)]|^2)}$, indicating the terms that are really related to the concentration of methane.

At the beginning time t_0, the concentration of methane is assumed to be 0 ppm denoted by $d(t_0) = 0$. In this case, at the specified frequency *f*, there is no band-gap, the amplitude of t is $Y_d[f, d(t_0)]$. At the moment *t*, the concentration of methane is increased to $d(t)$, in this case, at the specified frequency *f*, there is band-gap, and the amplitude of the band-gap is turned to be $Y_d[f, d(t)]$. The *identifiable sensitivity* of the sensor tag in terms of the amplitude modulation of band-gap frequency is defined as:

$$S_{amp}[d(t)](dB) = 20\lg\{\frac{Y_d[f, d(t)] - Y_d[f, d_0(t)]}{Y_d[f, d_0(t)]}\}. \quad (6)$$

Similarly at the beginning t_0, the concentration of methane is 0 ppm denoted by $d(t_0) = 0$, in this case, at the specified frequency f_0, there is band-gap, the value $Y_d[f_0, d(t_0)]$ is minimum as $f_0\{Y_d[f_0, d(t_0)]_{\min}\}$. At the moment *t*, the concentration of methane is increased to $d(t)$, in this case, at the specified frequency *f*, there is band-gap, the value $Y_d[f, d(t)]$ is minimum denoted by $f\{Y_d[f, d(t)]_{\min}\}$. The *identifiable sensitivity* of the sensor tag in terms of the frequency modulation of band-gap frequency is defined as:

$$S_{freq}[d(t)](dB) = 20\lg\{\frac{f\{Y_d[f, d(t)]_{mim}\} - f_0\{Y_d[f_0, d(t_0)]_{mim}\}}{f_0\{Y_d[f_0, d(t_0)]_{mim}\}}\}. \quad (7)$$

B. Sensor head

As the characteristics of the electromagnetic interface mentioned above, the sensor head should be the kind that can control either the amplitude or the frequency of the band-gap frequency according to the data of the concentration of methane in its vicinity. However, since the molecule of the methane (CH_4) is lower in the quality of polarity, it is difficult to find an exact mechanism used to detect methane through the way of molecule absorption and desorption [18], [19] till the time that a few of innovative solutions had been reported in some recent literatures [20-22]. The most interesting contribution was dedicated by Lu *et al.* who dispersed a Pd-SWCNTs bundle onto an interdigitated finger electrodes (IDE), delivering an architecture of sensor head that is qualified for detecting methane at room temperature. When this sensor head is exposed to methane gas, the materials of Pd-SWCNTs commence to interact with the methane's molecule, the equivalent conductance of the Pd-SWCNTs and the corresponding current across IDE electrodes as results can be changed with the change of the concentration of methane. The curve plotted in Fig. 2 shows that the current will be increased from 1.80 mA to 1.91 mA when the the concentration of methane is increased from 0 ppm to 100 ppm [22].

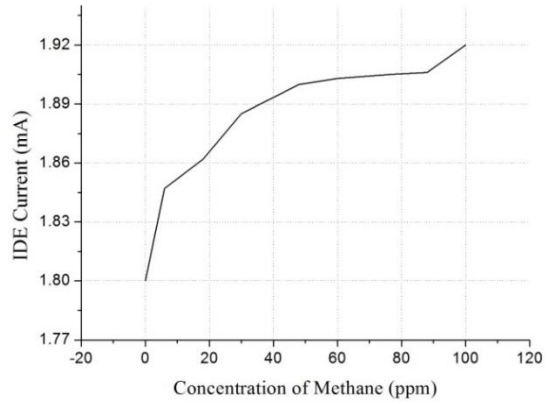

Fig. 2. Current flowing IDE versus the concentration of methane

IV. GEOMETRY OF CHIPLESS TAG

As discussed above, the intended sensor tag is the combination of an electromagnetic interface with a sensor head made from IDE loaded by Pd-SWCNTs. As shown in Fig. 3, there is one sensor head embedded in the middle location of the U-slot with one IDE electrodes soldered on the metallic plane close to the upper edge, and another IDE electrode soldered on the metallic plane close to the low edge of the U-slot. This implementation of the sensor tag is based on the scheme of the amplitude modulation of band-gap frequency. The size of this geometry guarantees the sensor tag be able to cover the entire UWB band with range from 3.1 GHz to 10.6 GHz; in the meanwhile, it has a band-gap at 5 GHz.

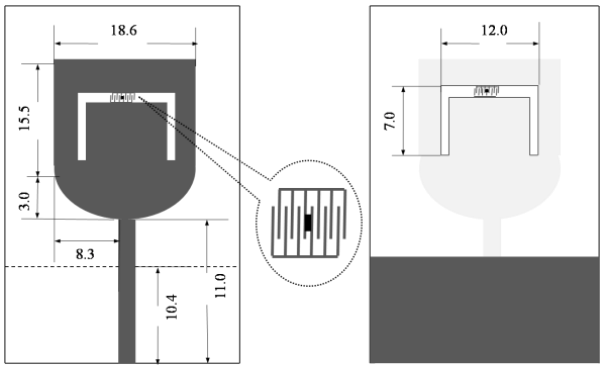

Fig. 3. (a) The front geometry of the proposed tag that the IDE loaded by Pd-SWCNTs is embedded in the middle of the U-slot, detecting methane based on the scheme of amplitude modulation of band-gap frequency. (b) Back of the proposed tag. (unit: mm)

Similarly, two identical sensor heads are embedded in the vertical arms of the U-slot symmetrically with a few distances away from the slot terminal ends, as shown in Fig. 4. This implementation of the sensor tag is based on the scheme of the frequency modulation of band-gap frequency. The size of this geometry guarantees the sensor tag to cover the entire UWB band, and having a band-gap frequency that can be shifted from 5 GHz to 5.25 GHz to reflect the concentration of methane increased from 0 ppm to 100 ppm.

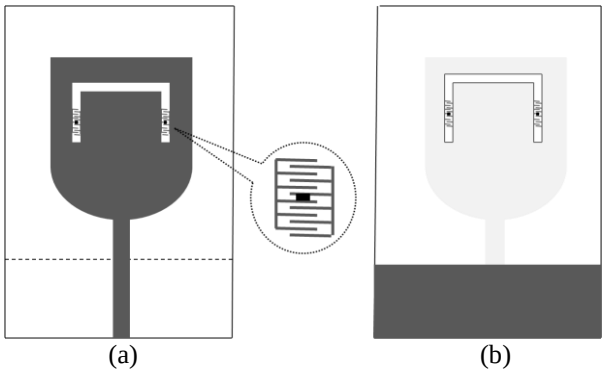

Fig. 4. (a) The front geometry of the proposed tag that the IDE loaded by Pd-SWCNTs is embedded in the vertical arms of the U-slot, detecting methane based on the scheme of frequency modulation of band-gap frequency. (b) Back of the proposed tag.

V. NUMERICAL APPROXIMATES, ANALYSES AND VALIDATION

The performance of the proposed sensor tags are described by the parameters of *identifiable sensitivity* as defined above. The process will be an approximate combination of the analytical and numerical method. In the analytical expression (6) and (7), the RCS σ and S_{22} will be achieved by numerical method or by real-field measurement.

The IDE with load of Pd-SWCNTs is regarded as a standalone component in the simulation model that will be replaced by an equivalent resistance achieved by simulation on the band-gap frequency. The simulation model of the sensor tag is based the fast multipole method algorithm (FMMA) in the consideration of that the operating frequency of the sensor tag is UWB band with range from 3.1 GHz to 10.6 GHz, the minimum wavelength is around 3 mm, comparatively smaller than the average size of the antenna dimension; Moreover, the FMMA can be applied to accelerate the iterative solver in the method of moments (MOM) as applied to the scattering problems about the computational electro-magnetic such as the computation of the RCS σ as it is required in this design [23].

With respect to the sensor tag illustrated in Fig. 3, the curve of the modulus of S_{22} versus frequency is shown in Fig. 5. It can be seen that there is a band-gap at 5 GHz. The modulus of S_{22} at the band-gap frequency is -7.73 dB, indicating the concentration of methane is 0 ppm (solid black line); while the modulus of S_{22} is changed to

-9.98 dB, indicating the concentration of methane is increased to 100 ppm (dash dot red line), the discrepancy is achieved by 2.25 dB.

The curve of RCS versus frequency is shown in Fig. 6. When the concentration of methane is 0 ppm, the RCS at the band-gap frequency is -32.59 dBsm (solid black line); however, when the concentration of methane is increased to 100 ppm, this RCS is decreased to -31.61 dBsm (dash dot red line), the discrepancy is 0.98 dB.

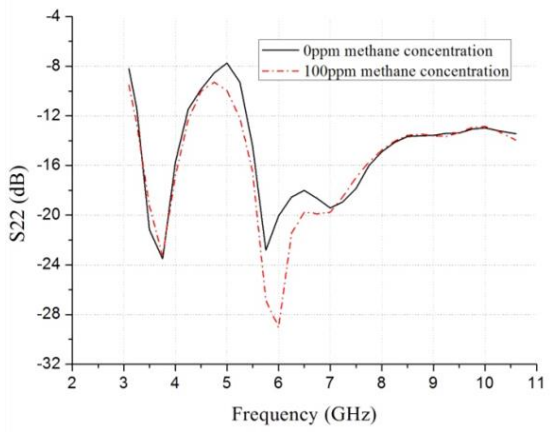

Fig. 5. S_{22} versus the concentration of methane and the frequency upon the scheme of amplitude modulation of band-gap frequency.

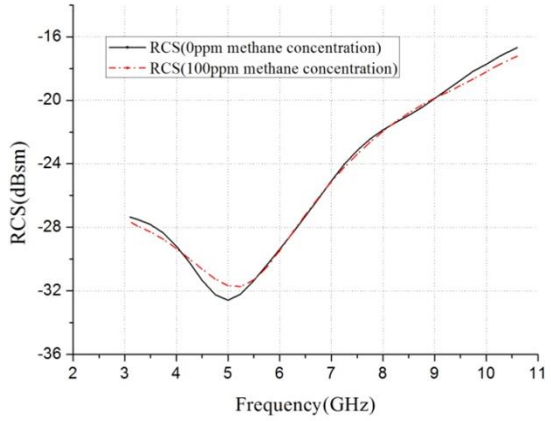

Fig. 6. RCS versus the concentration of methane and the frequency upon the scheme of amplitude modulation of band-gap frequency.

Substituting these values into (6), we can achieve the parameter of the *identifiable sensitivity* by -9.32 dB to specify that the concentration of methane is 100 ppm, as shown in Fig. 7.

With respect to the sensor tag illustrated in Fig. 4, the curve of the modulus of S_{22} versus frequency is shown in Fig. 8. The band-gap is at 5 GHz for the concentration of methane by 0 ppm (solid black line). This band-gap is moved to 5.25 GHz for the concentration of methane increased to 100 ppm (dash dot red line). When the concentration of methane is increased from 0 ppm to 100 ppm, the minimum RCS is moved from 6.45 GHz to 6.75 GHz, as shown in Fig. 9.

Substituting all these values into $Y_d[f, d(t)] = \eta_L[d(t)]\sqrt{1 - |S_{22}[f, d(t)]|^2}$, we can get $Y_d[f, d(t)]$ versus frequency as shown in Fig. 10. When the concentration of methane is 0 ppm, the minimum $Y_d[f, d(t)]$ is achieved at the frequency of 6.25 GHz (solid black line); but when the concentration is increased to 100 ppm, the minimum $Y_d[f, d(t)]$ is moved to the frequency of 6.75 GHz (dash dot red line).

Substituting these values into (7), we can achieve the *identifiable sensitivity* by -11.30 dB for the methane concentrated by 100 ppm, as shown in Fig. 11.

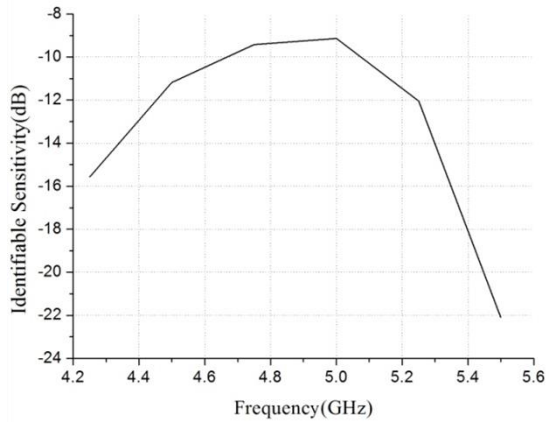

Fig. 7.The identifiable sensitivity for the concentration of methane of 100 ppm upon amplitude modulation of band-gap frequency.

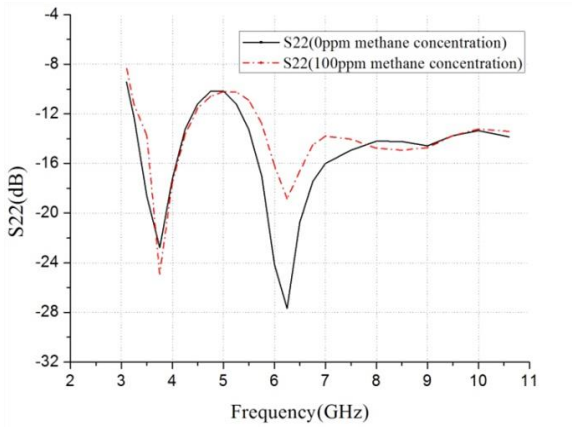

Fig. 8. S_{22} versus the concentration of methane and frequency in terms of the scheme of frequency modulation of band-gap frequency.

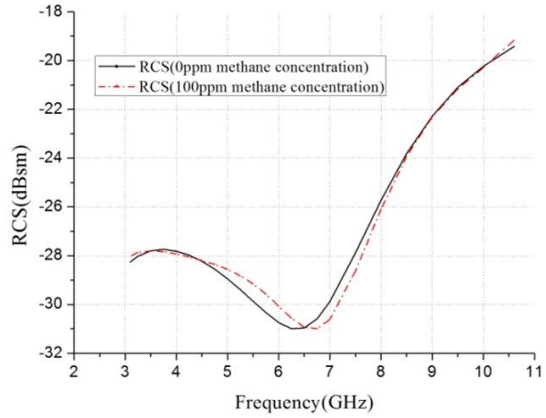

Fig. 9. RCS versus the concentration of methane and the frequency in terms of the scheme of frequency modulation of band-gap frequency.

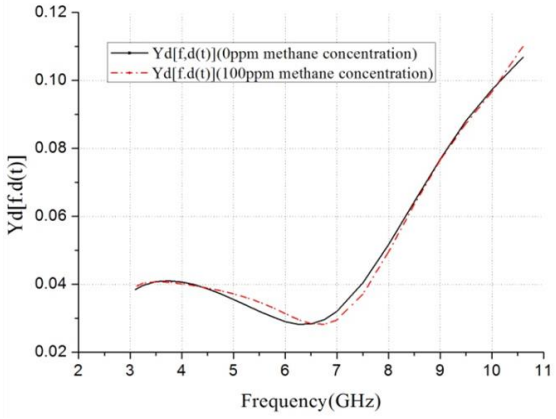

Fig. 10. $Y_d[f, d(t)]$ versus the concentration of methane and the frequency in terms of the scheme of frequency modulation of band-gap frequency.

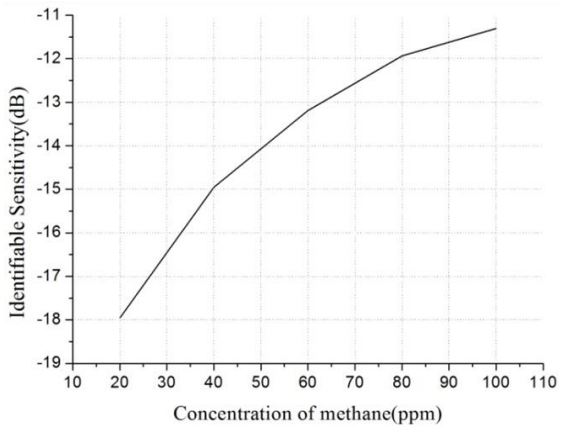

Fig. 11. The identifiable sensitivity achieved in terms of the scheme of the frequency modulation of band-gap frequency.

VI. CONCLUSION

It can be concluded form this design that the Pd-SWCNTs enabled UWB-RFID chiplees sensor can be used to conduct the detection of concentration of methane at room temperature. Based on the structural mode of the backscattering signal, the geometry of sensor tag is simple and the detection procedure is cost efficient.

It can be seen that band-gap can be introduced by etching U-slot on the planar antenna of UWB. The band-gapped frequency can be designated as the sensing signature. If the amplitude of the band-gap frequency is manipulated by the data of the concentration of methane, it forms the scheme of the amplitude modulation of band-gap frequency; and if the frequency of band-gap frequency is manipulated by the data of the concentration of methane, it forms the scheme of the frequency modulation of band-gap frequency.

The performance of the proposed sensor tag is validated by a method combing the analytical and numerical computation with deliverables of the parameter of *identifiable sensitivity* that is achieved by -9.32 dB in terms of the scheme of amplitude modulation of band-gap frequency, or by -11.30 dB in terms of the scheme of frequency modulation of band-gap frequency, indicating the methane concentrated by 100 ppm at room temperature.

It is evidence that the dynamic range of the identifiable sensitivity is quite constraint due to the limitation of Pd-SWCNTs. The performance of the sensor tag would be improved when more advanced nano-materials in specific for the detection of methane can be available in future.

REFERENCES

[1] D. Kohl, "Function and application of gas sensors," *J. Phys. D Appl. Phys.*, vol. 34, pp. 125-149, 2001.

[2] C. Occhiuzzi, A. Rida, G. Marrocco, and M. Tentzeris, "RFID passive gas sensor integrating carbon nanotubes," *Microwave Theory and Techniques, IEEE Transactions on*, vol. 59, no. 10, pp. 2674-2684, Oct. 2011.

[3] V. Chawla and D. S. Ha, "An overview of passive RFID," *IEEE Commun. Mag.*, vol. 45, no. 9, pp. 11-17, Sep. 2007.

[4] V. Plessky and L. Reindl, "Review on SAW RFID tags," *IEEE Trans. Ultrason. Ferroelectr. Freq. Contro.*, vol. 57, no. 3, pp. 654-668, 2010.

[5] D. Girbau, J. Lorenzo, A. Lazaro, C. Ferrater, and R. Villarino, "Frequency coded chipless RFID tag based on dual-band resonators," *IEEE Antennas and Wireless Propagation Letters*, vol. 11, pp. 126-128, 2012.

[6] I. Balbin and N. C. Karmakar, "Phase-encoded chipless RFID transponder for large-scale low-cost

applications," *IEEE Microwave Wireless Compon. Lett.*, vol. 19, no. 8, pp. 509-511, Aug. 2009.

[7] B. Shao, Q. Chen, R. Liu, and L. R. Zheng, "Design of fully printable and configurable chipless RFID tag on flexible substrate," *Microwave and Optical Technology Letter*, vol. 54, no. 1, pp. 226-230, 2012.

[8] K. Finkenzeller, *RFID Handbook: Fundamentals and Applications in Contactless Smart Cards and Identification*. 2nd ed., New York: Wiley, 2004.

[9] D. Dardari, R. D'Errico, C. Roblin, A. Sibille, and M. Z. Win, "Ultrawide bandwidth RFID: The next generation?," *Proc. IEEE*, vol. 98, no. 9, pp. 1570-1582, Sep. 2010.

[10] S. Hu, Y. Zhou, C. L. Law, and W. Dou, "Study of a uniplanar monopole antenna for passive chipless UWB-RFID localization system," *IEEE Trans. Antennas Propag.*, vol. 58, no. 2, pp. 271-278, Feb. 2010.

[11] D. Girbau, Á. Ramos, A. Lázaro, S. Rima, and R. Villarino, "Passive wireless temperature sensor based on time-coded UWB chipless RFID tags," *IEEE Trans. Mircow. Theory Tech.*, vol. 60, no. 11, pp. 2623-2632, Nov. 2012.

[12] Y. F. Weng, S. W. Cheung, T. I. Yuk, and L. Liu, "Design of chipless UWB RFID system using a CPW multi-Resonator," *IEEE Antennas. Propag. Mag.*, vol. 55, no. 1, pp. 13-31, Feb. 2013.

[13] A. Ramos, A. Lazaro, D. Girbau, and R. Villarino, "Time-domain measurement of time-coded UWB chipless RFID tags," *Progress in Electromagnetics Research*, vol. 116, pp. 313-331, 2011.

[14] Federal Communications Commission, Revision of Part 15 of the Commission's Rules Regarding Ultra-Wideband Transmission Systems, First Rep. Order (ET Docket98–153), Adopted Feb. 14, 2002. Released Apr. 22, 2002.

[15] Z. Chen, X. Wu, H. Li, N. Yang, and M. Y. W. Chia, "Considerations for source pulses and antennas in UWB radio systems," *IEEE Trans. Antennas Propag.*, vol. 52, no. 7, pp. 1739-1748, July 2004.

[16] C. A. Balanis, *Antenna Theory Analysis and Design*. 3rd ed., Hoboken, NJ: Wiley, 2005.

[17] E. A. Daviu, M. C. Fabrés, M. F. Bataller, and V. M. R. Peñarrocha, "Modal analysis and design of band-notched UWB," *IEEE Trans. Antennas Propag.*, vol. 58, no. 5, pp. 1453-1467, May 2010.

[18] R. Bogue, "Nanomaterials for gas sensing: A review of recent research," *Sensor Review*, vol. 34, no. 1, pp. 1-8, 2014.

[19] J. Chen, M. A. Hamon, H. Hu, Y. Chen, A. M. Rao, P. C. Eklund, and R. C. Haddon, "Solution properties of single-walled carbon nanotubes," *Science*, vol. 282, pp. 95-98, 1998.

[20] Z. P. Li, J. F. Li, X. Wu, S. M. Shuang, C. Dong, and M. M. F. Choi, "Methane sensor based on nanocomposite of palladium/multi-walled carbon nanotubes grafted with 1,6-hexanediamine," *Sensors and Actuators B*, vol. 139, pp. 453-459, 2009.

[21] A. Biaggi-Labiosa, F. Sola, M. Lebron-Colon, L. J. Evans, J. C. Xu, G. W. Hunter, G. M. Berger, and J. M. Gonzalez, "A novel methane sensor based on porous SnO2 nanorods: Room temperature to high temperature detection," *Nanotechnol.*, vol. 23, pp. 455-501, 2012.

[22] Y. Lu, J. Li, J. Han, H. T. Ng, C. Binder, C. Partridge, and M. Meyyappan, "Room temperature methane detection using palladium loaded single-walled carbon nanotube sensors," *Chem. Phys. Lett.*, vol. 391, pp. 344-348. 2004.

[23] E. Nader, D William, V. R. Murphy, O. Ladimir, and V. Marius, "The fast multipole method for electromagnetic scattering computation," *IEEE Transactions on Antennas and Propagation*, vol. 40, pp. 634-641, 1992.

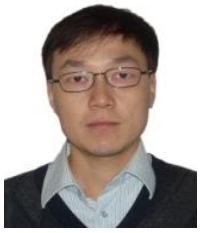

Jian Liu was born in Xi'an, Shaanxi, in 1967. He received the B.S. and M.S. degrees in the Electromagnetic Field Engineering from Xidian University, Xi'an, in 1990 and 1996. From 1990 to 1996, he was an Assistant Professor with the Communication Engineering Department, Xi'an Mining Institute. From 1997 to 1998, he was an Electrical Engineer with RF & Wireless Laboratory, ZTE. From 1998 to 2000, he was a Lecturer with the Communication Engineering Department, Xi'an Science and Technology College. From 2000 to 2003, he was the Senior Scientist and Project Leader with Philips Research Laboratory. From 2004 to 2010, he was Department Head of PTCC, Panasonic Research and Development Cooperation Limited. Since 2010, he has been a Lecturer with the School of Communication and Information Engineering, Xi'an University of Science and Technology. He is the author of 1 text book, more than 10 articles, and holds 7 patents. His research interests include Computational Electromagnetism, Antenna, RF & Microwave Communication and Sensors.

Baiping Li received the B.S., M.S. and Ph.D. in 1985, 1997 and 2011 from Chongqing University, Liaoning Technical University and Xi'an University of Science and Technology, respectively. She is now the Professor and the Head of the School of Communication and Information Engineering, Xi'an University of Science and Technology. She is the author of six books, and more than 40 articles. Her research interests include the key technologies on Wireless Communications and Sensor Networks.